An Efficient Multi-Beam Pattern Measurement Campaign for Millimeter-Wave Phased Arrays

Gao, Huaqiang; Zhang, Fengchun; Pedersen, Gert Frølund; Fan, Wei

Published in:
17th European Conference on Antennas and Propagation, EuCAP 2023

DOI (link to publication from Publisher):
10.23919/EuCAP57121.2023.10133520

Publication date:
2023

Document Version
Accepted author manuscript, peer reviewed version

An Efficient Multi-Beam Pattern Measurement Campaign for Millimeter-Wave Phased Arrays

Huaqiang Gao[1], Fengchun Zhang[1], Gert Frølund Pedersen[1], Wei Fan[1,2]
[1]Department of Electronic Systems, Aalborg University, Aalborg, Denmark, gaohq@ieee.org
[2]Center for Wireless Communication-Radio Technology (CWC-RT), University of Oulu, Oulu, Finland, wfa@es.aau.dk

***Abstract*—The performance of millimeter-wave (mmWave) radio systems depends on accurate knowledge of mmWave phased array multi-beam patterns. However, the conventional antenna pattern measurement methods are inefficient for mmWave multi-beam measurements. To solve the problem, a fast multi-beam reconstruction method has been proposed in the literature. Based on that, this paper conducts an efficient multi-beam pattern measurement campaign for a practical 4×4 mmWave phased array antenna-in-package (AiP). The measurement results show that the element patterns of an active phased array AiP measured in the on-off and all-on modes might differ, especially for large-scale arrays. Furthermore, the reconstructed array multi-beam patterns by the proposed method are compared with the conventional compact antenna testing range (CATR) measurement data. The all-on reconstructed array multi-beam patterns matches better with the target array patterns than the on-off reconstructed array patterns.**

***Index Terms*—Antenna measurement, beam-steering, element pattern, millimeter-wave (mmWave) phased array, multi-beam.**

I. Introduction

Millimeter-wave (mmWave) phased arrays have been widely employed in mmWave communication systems due to their capability to generate a beam of radio waves that can be electronically steered to different directions [1]. The over-the-air (OTA) conformance test of mmWave phased arrays with integrated antenna-in-package (AiP) design in 5G mmWave user equipment (UE) and base station (BS) devices is a mandatory requirement according to 3GPP specifications [2]–[4]. For the testing, a precise characterization of the device performance under far-field conditions is necessary. In particular, the antenna pattern and key parameters of the antenna pattern, e.g. main beam, sidelobes, and nulls, are crucial to the performance of radio systems. Moreover, the knowledge of antenna array element pattern can provide insights to the phased array design and development.

The literature has a thorough investigation of the conventional antenna pattern measurements with various antenna ranges [5]–[9], which are inefficient for the multi-beam measurements of mmWave beam-steerable phased arrays [10]. Reference [10] has proposed a fast multi-beam pattern reconstruction method for mmWave phased arrays. The proposed method can rapidly reconstruct the multi-beam patterns of phased array based on the measured element patterns. Different from the conventional element pattern measurement where each element is excited individually (i.e. in an on-off mode), the proposed method retrieves the element pattern in the normal all-on working mode of phased arrays (i.e. with all elements excited). In [11], all element patterns in a hybrid beamforming array are simultaneously obtained using an orthogonal code-based measurement method. An extra pulse generator with multiprobe is used for coding and needs to be integrated into the measurement system, which is more complicated than the conventional antenna measurement facilities. More importantly, the method in [11] requires individual array element ports connected to the pulse generator, which can be applied only in digital and hybrid beamformed arrays. Similar work was reported in [12], which only works for antenna systems with digital beamformer structure. For the array with a hybrid beamforming structure, the element pattern in an analog beamformed sub-array still cannot be obtained. Compared with [11], reference [10] is focused on pattern measurement methods applicable for analog structure, though its principle can be directly applied for digital and hybrid structures.

Based on [10], this paper conducts an efficient multi-beam pattern measurement campaign for mmWave phased arrays. The rest of this paper is organized as follows. In Section II, the measurement setup utilized in the measurement campaign is described. The measurement procedures are compared between the conventional and the proposed methods in Section III. Measurement results are shown in Section IV. Section IV concludes the paper finally.

II. Measurement Setup

In the measurement campaign, a 4×4 mmWave phased array AiP described in [13] was used. Based on a standard compact antenna testing range (CATR) setup at Aalborg University, Denmark, the multi-beam pattern measurement method proposed in [10] was validated by a measurement campaign in this paper. The AiP and the CATR setup operate from 26.5 GHz to 29.5 GHz, and from 6 GHz to 60 GHz, respectively. An anechoic chamber, a feed antenna, a reflector, and a turntable are mainly included in the CATR setup.

The measurement setup composed of the AiP and the CATR setup is shown in Fig. 1. With the polarization of feed antenna and AiP aligned, the AiP was placed in the quiet zone of the CATR setup where the far-field plane wave condition is satisfied. The transmission S-parameter measurements between the feed antenna port and the AiP port were conducted via a vector network analyzer (VNA). With the AiP operating in receive

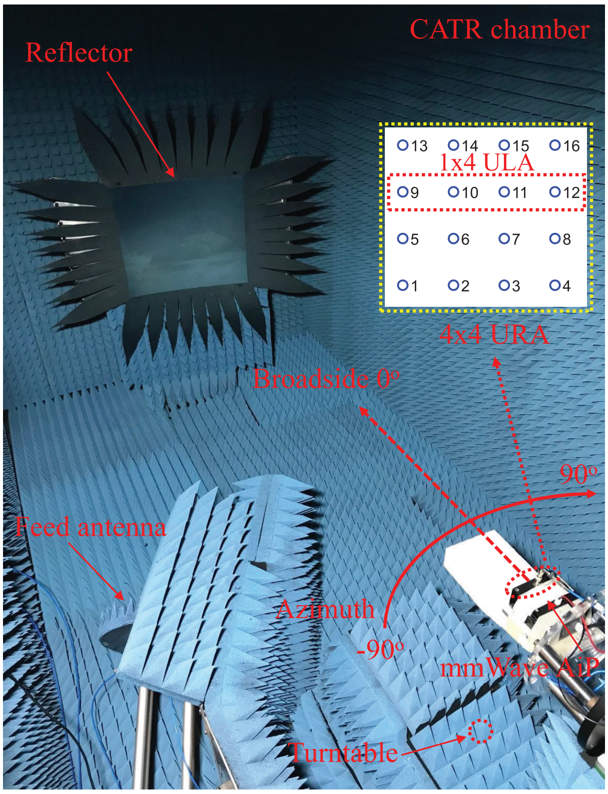

Fig. 1. A photograph of measurement setup in a CATR chamber. The VNA and a computer installed with the control program are outside the chamber.

mode, the transmit and receive ports of VNA were connected to the feed antenna port and the AiP port, respectively. The S-parameters in different far-field observation directions of the AiP were recorded with the AiP rotation in the CATR setup. Conventionally, the element and array patterns were recorded by the S-parameters that are directly measured in the on-off mode and the all-on mode, respectively. In the proposed method in [10], however, the S-parameters measured in the all-on mode were used to retrieve the element pattern without turning on and off elements.

III. Measurement Procedure

The AiP antenna configuration is a 4×4 uniform rectangular array (URA) that consists of 4 horizontal 1×4 ULAs distributed in the vertical direction, as shown in Fig. 1. In the following measurement campaign, the ULA marked in Fig. 1 and URA were independently investigated for 7 beams with horizontal beam-steering angles $0°$, $\pm 17°$, $\pm 35°$, and $\pm 59°$, as an example.

A. Conventional Pattern Measurement

Conventionally, the AiP element pattern and array pattern were directly measured at 28 GHz in the standard CATR setup where a constant step of $1°$ was used to rotate the AiP in a horizontal direction with an azimuth angle from $-90°$ to $90°$. The AiP position shown in Fig. 1 with the broadside direction pointing to the CATR reflector center was indicated by the azimuth angle of $0°$. After the entire horizontal rotation of AiP has been completed, a horizontal pattern cut over azimuth angles inside $[-90°, 90°]$ has been recorded. The 4 and 16 element patterns in the ULA and URA without beam-steering were directly measured with one element activated each time while the others deactivated, respectively, i.e. the conventional on-off measured element patterns. The target array patterns for comparison were directly measured in the all-on mode of both arrays steered to 7 beams (i.e. $0°$, $\pm 17°$, $\pm 35°$, and $\pm 59°$).

B. Proposed Pattern Measurement

The system hardware used for the proposed pattern measurement is the same as for the conventional measurement. Instead, a constant step of $5°$ was used to rotate the AiP in a horizontal direction with an azimuth angle from $-90°$ to $90°$. Assuming AiP elements with initial phase shift settings of $0°$ at each azimuth angle, 5 and 17 S-parameter measurements for 5 and 17 extra phase shift settings of elements according to [10] were recorded for the ULA and URA, respectively. After the measurements of S-parameters for all azimuth angles has been completed, the element patterns measured in the all-on mode were obtained, i.e. the proposed all-on measured element pattern. The array patterns were reconstructed by summing up the all-on measured element patterns without and with beam-steering weights for the broadside beam ($0°$) and the steered beams ($\pm 17°$, $\pm 35°$, and $\pm 59°$), respectively, i.e. the all-on reconstructed array patterns. Similarly, the on-off reconstructed array patterns sum up the on-off measured element patterns in the conventional measurement. The on-off and all-on reconstructed array patterns were compared with the target array patterns measured in the conventional measurement for validation.

IV. Measurement Results

A. Array Element Patterns

The on-off and all-on measured element patterns with an angle step of $5°$ are shown in Fig. 2 for both arrays. The common elements in both arrays (i.e. element index 9, 10, 11, 12 marked in Fig. 1) are investigated, i.e. the on-off measured element patterns are the same for both arrays since the ULA is selected from the URA. The element patterns in both arrays are not smooth, which is different from simulations. This might be due to the effects of element coupling and amplifiers in active phased arrays. The element patterns measured in the on-off and all-on modes of the ULA are matched better than the URA. One of reasons is that the AiP chip temperature might be different for the ULA and URA since the number of activated elements are different between both arrays. The chip temperature of the ULA with 4 elements activated is similar to that with one element activated (i.e. the on-off mode, around $40\,°\mathrm{C}$), while the temperature of the URA with 16 elements activated is around $100\,°\mathrm{C}$. The temperature affects the amplifier response in element branches, as discussed in [13]. Therefore, the element patterns measured in on-off and all-on modes could be different for an active phased array AiP. The difference will be larger with the increase of array scale.

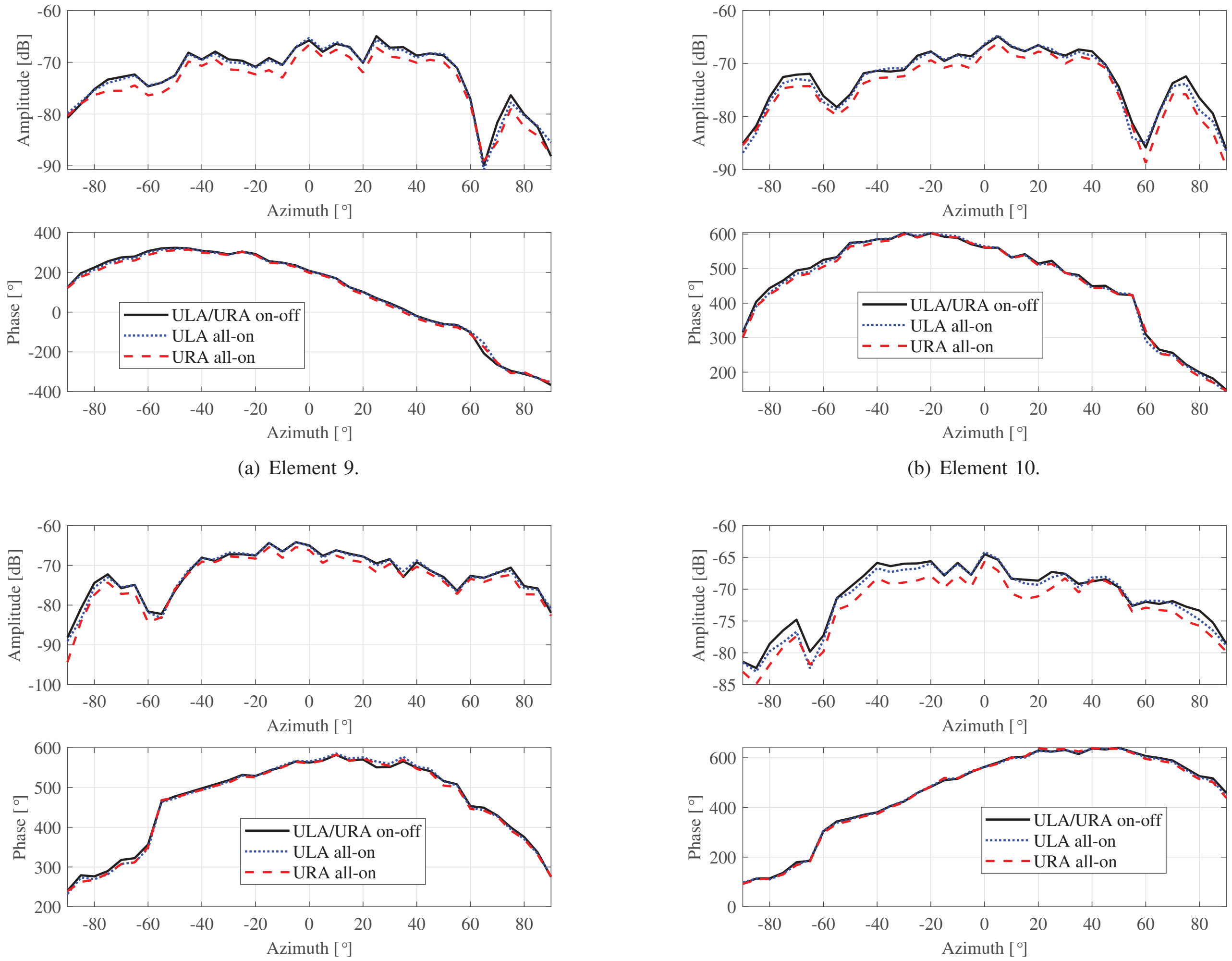

(a) Element 9. (b) Element 10.

(c) Element 11. (d) Element 12.

Fig. 2. Element patterns measured in the on-off and all-on modes for both arrays.

B. Array Multi-Beam Patterns

The power patterns of the ULA and URA for 7 beams are shown in Fig. 3 and Fig. 4, respectively. The all-on reconstructed array patterns matches well with the target array patterns for both arrays regarding the main beam direction and power, while the on-off reconstructed array patterns match well with the target only for the ULA. For example, 1.5-dB amplitude error between the target and on-off reconstructed array patterns can be observed in the main beam peak direction for the broadside beam of URA. It can be found that the on-off reconstructed array pattern is not the actual array pattern in the all-on working mode for 7 beams, which emphasizes the importance of element pattern measurement in an all-on mode for the efficient multi-beam measurement.

C. Sparse Measurement Sampling

To further demonstrate the efficiency of measurement campaign, the number of sampling angles within $[-90°, 90°]$ is reduced from 181 points with a uniform step of $1°$ to 19 points with a uniform step of $10°$ and to 7 points with a uniform step of $30°$. Reducing the number of sampling angles can reduce the number of required mechanical rotations in the existing hardware setup or reduce the number of required probes in a multi-probe setup. Taking the URA for example, the all-on measured element patterns sampled with an angle step of $10°$ and $30°$ are obtained first, then the sampled element patterns are interpolated with an angle step of $1°$. In the end, the beam-steering weights from various beams and the interpolated element patterns are combined to reconstruct various array patterns with an angle step of $1°$. The array patterns reconstructed by $10°$ and $30°$ angle sampling steps are compared with the target array pattern with an angle step of $1°$ in Fig. 5 for beams $0°$, $-17°$, $-35°$, and $-59°$, respectively. The two angle sampling steps achieve the same main beam pattern as the target for 4 beams, though error exists in terms of sidelobes and nulls. The errors of sidelobes and nulls achieved by $10°$ sampling are smaller than those by $30°$ sampling. Note that a trade off between the sparse

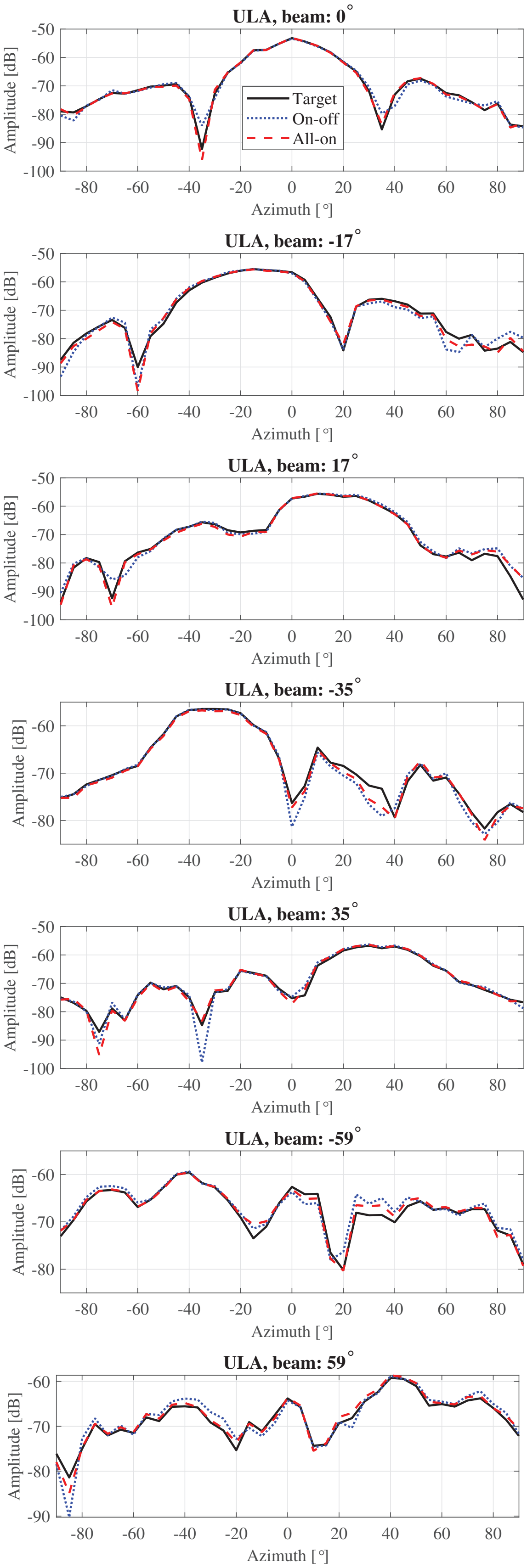

Fig. 3. ULA pattern comparison between the target and the reconstructed for 7 beams.

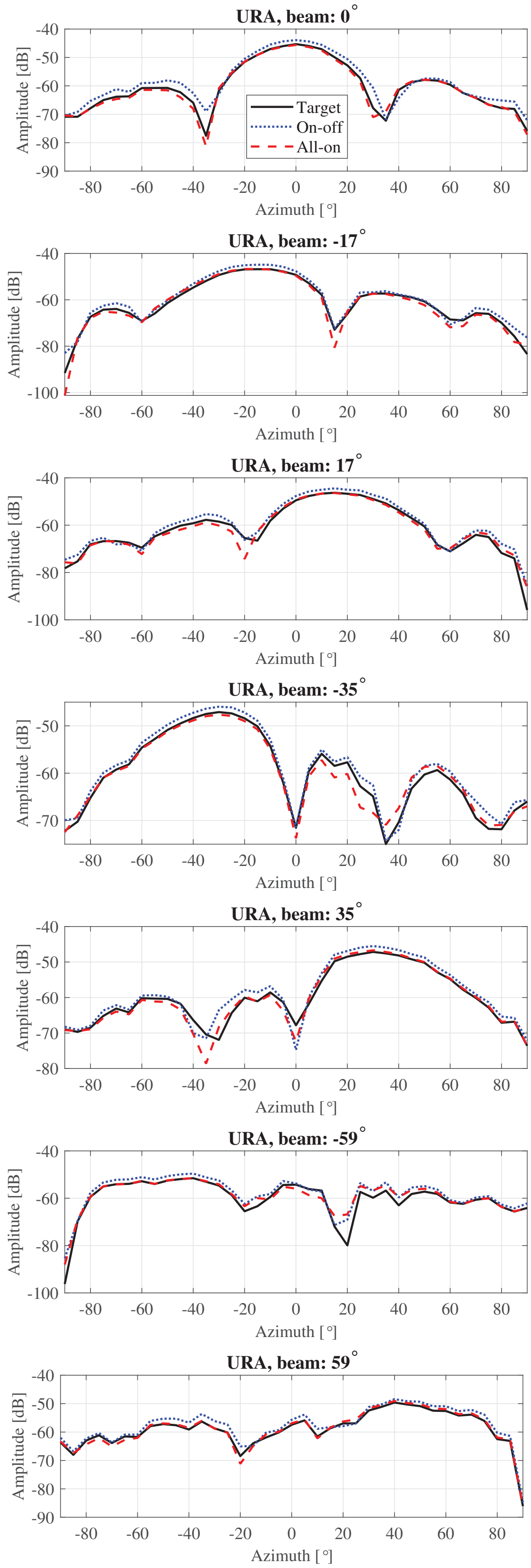

Fig. 4. URA pattern comparison between the target and the reconstructed for 7 beams.

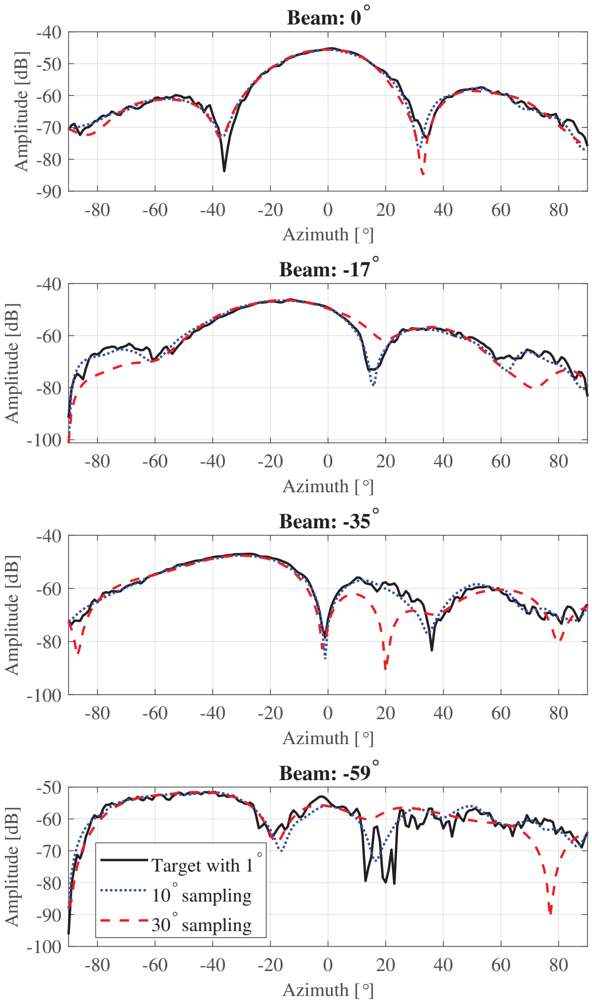

Fig. 5. URA pattern comparison between the target and the all-on reconstructed using two element pattern sampling steps for 4 beams.

sampling step and the pattern accuracy should be considered according to applications. For example, the main beam is the focus in mmWave UE applications where a sparse angle sampling can be adopted. For those applications where accurate measurements of sidelobes and nulls are also required, e.g. mmWave BS, the sampling step will be decreased for more accurate pattern performance.

V. Conclusion and Future Work

In this paper, an efficient multi-beam pattern measurement campaign has been presented using a fast multi-beam pattern measurement method of mmWave phased array antenna systems. In the measurement campaign, all element complex patterns in practical all-on mode of arrays can be retrieved accurately for multi-beam pattern reconstruction of phased arrays. Moreover, the multi-beam array patterns can be reconstructed more efficiently by a sparse sampling of element patterns with wide beamwidth. For future work, it would be desirable to extend the measurement method based on a near-field setup with reduced measurement distance. In this case, the free space propagation coefficients between array elements and probes need to be carefully calibrated out from the measured element fields. Besides, the complex measurement requirement might be challenging due to the inaccessible antenna connectors and the difficulties of phase measurement at mmWave frequencies. Therefore, it would be also desirable to retrieve the element complex pattern by amplitude-only measurements in practical mmWave systems.

Acknowledgment

This work was partially supported by the 21NRM03 MEWS project, which has received funding from the European Partnership on Metrology, co-financed from the European Union's Horizon Europe Research and Innovation Programme and by the Participating States.

References

[1] W. Roh, J.-Y. Seol, J. Park, B. Lee, J. Lee, Y. Kim, J. Cho, K. Cheun, and F. Aryanfar, "Millimeter-wave beamforming as an enabling technology for 5G cellular communications: Theoretical feasibility and prototype results," *IEEE Communications Magazine*, vol. 52, no. 2, pp. 106–113, 2014.

[2] Y. Zhang and J. Mao, "An overview of the development of antenna-in-package technology for highly integrated wireless devices," *Proceedings of the IEEE*, vol. 107, no. 11, pp. 2265–2280, 2019.

[3] TS 38.521-2, "NR; User Equipment (UE) conformance specification; Radio transmission and reception; Part 2: Range 2 standalone," 3GPP, Technical Specification, V17.0.0, October 2022.

[4] TS 38.141-2, "NR; Base Station (BS) conformance testing Part 2: Radiated conformance testing," 3GPP, Technical Specification, V17.7.0, September 2022.

[5] H. T. Friis, "A note on a simple transmission formula," *Proceedings of the IRE*, vol. 34, no. 5, pp. 254–256, 1946.

[6] S. Costanzo, G. Di Massa, and M. D. Migliore, "A novel hybrid approach for far-field characterization from near-field amplitude-only measurements on arbitrary scanning surfaces," *IEEE Transactions on Antennas and Propagation*, vol. 53, no. 6, pp. 1866–1874, 2005.

[7] M. Shields, "The compact RCS/antenna range at MIT Lincoln laboratory," in *2009 3rd European Conference on Antennas and Propagation*. IEEE, 2009, pp. 939–943.

[8] H. Kong, Z. Wen, Y. Jing, and M. Yau, "Midfield over-the-air test: A new OTA RF performance test method for 5G massive MIMO devices," *IEEE Transactions on Microwave Theory and Techniques*, vol. 67, no. 7, pp. 2873–2883, 2019.

[9] F. Scattone, D. Sekuljica, A. Giacomini, F. Saccardi, A. Scannavini, L. Foged, E. Kaverine, N. Gross, and P. Iversen, "OTA testing of antennas & devices using plane wave generator or synthesizer," in *14th European Conference on Antennas and Propagation, EuCAP*, 2020.

[10] H. Gao, F. Zhang, G. F. Pedersen, and W. Fan, "A fast multibeam measurement method for millimeter-wave phased arrays," *IEEE Antennas and Wireless Propagation Letters*, vol. 21, no. 7, pp. 1502–1506, 2022.

[11] S. Park, H.-S. Lee, and J.-G. Yook, "Orthogonal code-based transmitted radiation pattern measurement method for 5G massive MIMO antenna systems," *IEEE Transactions on Antennas and Propagation*, vol. 68, no. 5, pp. 4007–4013, 2020.

[12] Y. Ji, J. Ø. Nielsen, and W. Fan, "Simultaneous wideband calibration for digital beamforming array at short distance," *IEEE Antennas and Propagation Magazine*, 2021.

[13] H. Gao, W. Wang, W. Fan, F. Zhang, Z. Wang, Y. Wu, Y. Liu, and G. F. Pedersen, "Design and experimental validation of automated millimeter-wave phased array antenna-in-package (AiP) experimental platform," *IEEE Transactions on Instrumentation and Measurement*, vol. 70, pp. 1–11, 2020.